Photoluminescence and Quantum Yields of Urea and Urethane Cross-Linked Nanohybrids Derived from Carboxylic Acid Solvolysis

Lianshe Fu, R. A. Sá Ferreira, N. J. O. Silva, and L. D. Carlos*

Departamento de Física, CICECO, Universidade de Aveiro, 3810-193 Aveiro, Portugal

V. de Zea Bermudez

Departamento de Química and CQ-VR, Universidade de Trás-os-Montes e Alto Douro, 5000-911 Vila Real Codex, Portugal

J. Rocha

Departamento de Química, CICECO, Universidade de Aveiro, 3810-193 Aveiro, Portugal

Received October 17, 2003. Revised Manuscript Received February 6, 2004

Urea and urethane cross-linked hybrids, classed as di-ureasils and di-urethanesils, were prepared through sol−gel derived carboxylic acid solvolysis. The resulting nanohybrids were characterized by X-ray diffraction, mid-infrared spectroscopy, ^{29}Si and ^{13}C nuclear magnetic resonance, and photoluminescence spectroscopy and results were compared with those of similar hybrid materials obtained from the conventional sol−gel route. The results indicate a similar structure for the hybrids, independent of the synthesis process used. All the hybrids are efficient room-temperature white-light emitters with emission quantum yields between 6 and 20%. The emission quantum yields of hybrids prepared through carboxylic acid solvolysis are 27−35% higher than those calculated for the di-ureasils and di-urethanesils synthesized via the conventional sol−gel technique. This is attributed to the presence of a larger number of nonbonded NH urea- and urethane-groups in the hybrids prepared by carboxylic acid solvolysis, illustrating the key role played by the synthetic method on the extent and magnitude of hydrogen bonding involving urea and urethane linkages.

I. Introduction

In the last two decades, the drive to miniaturization has been pushing industry into the atomic and nanometer scales requiring the development of new strategies for the synthesis of advanced materials. Among the available synthetic methods employed for the development of nanosystems, the sol−gel procedure presents advantages such as relatively low processing temperature, high purity, improvement of the thermal and dimensional stability of the resulting compounds, and ease of shaping the product into thin films, fibers, and monoliths.[1,2] Pure and well-controlled multifunctional organic−inorganic hybrids may be synthesized through a molecular nanotechnology "bottom-up" approach based on a tailored assembly of nanoscopic organic and inorganic building blocks. This opens up exciting new avenues in materials science and related technologies with significant implications in nanotechnological processing, which facilitate integration, miniaturization, and multifunctionalization of devices.[3−12] In particular, the sol−gel approach offers the flexibility necessary for implementing the chemical design strategies that are the basis of photonic hybrid materials, one of the most attractive fields for applications in the 21st century.[7,8,13−15]

The outgrowth of new full color displays that are cheaper and less aggressive to the global environment is one of the main challenging tasks for the next generation of flat-panel display systems and lighting technology. The hybrid concept has been recently employed to synthesize stable and efficient full-color luminescent siloxane-based organic−inorganic materials lacking metal activator ions.[16−28] Emphasis is given to amide- or

* Corresponding author. Phone: 351 234 370946. Fax: 351 234 424965. E-mail: lcarlos@fis.ua.pt.

(1) Hench, L. L.; West, J. K. *Chem. Rev.* **1990**, *90*, 33.
(2) Brinker, C. J.; Scherer, G. W. *Sol−gel Science: The Physics and Chemistry of Sol−Gel Processing*; Academic: San Diego, CA, 1990.
(3) Novak, B. M. *Adv. Mater.* **1993**, *5*, 422.
(4) Sanchez, C.; Ribot, F. *New J. Chem.* **1994**, *18*, 1007.
(5) Schubert, U.; Hüsing, N.; Lorenz, A. *Chem. Mater.* **1995**, *7*, 2010.
(6) Loy, D. A.; Shea, K. J. *Chem. Rev.* **1995**, *95*, 1431.
(7) Judeinstein, P.; Sanchez, C. *J. Mater. Chem.* **1996**, *6*, 511.
(8) Wen, J. Y.; Wilkes, G. L. *Chem. Mater.* **1996**, *8*, 1667.
(9) Sanchez, C.; Ribot, F.; Lebeau, B. *J. Mater. Chem.* **1999**, *9*, 35.
(10) Ahmad, Z.; Mark, J. E. *Chem. Mater.* **2001**, *13*, 3320.
(11) Mitzi, D. B. *Chem. Mater.* **2001**, *13*, 3283.
(12) Ben, F.; Boury, B.; Corriu, R. J. P. *Adv. Mater.* **2002**, *14*, 1081.
(13) Schmidt, H.; Jonschker, G.; Goedicke, S.; Mennig, M. *J. Sol-Gel Sci. Technol.* **2000**, *19*, 39.
(14) Sanchez, C.; Lebeau, B. In *Hybrid Organic−Inorganic Materials*; Loy, D. A., Ed.; *Mater. Res. Soc. Bull.* **2001**, *26*, 377.
(15) Scott, B. J.; Wirnsberger, G.; Stucky, G. D. *Chem. Mater.* **2001**, *13*, 3140.
(16) Green, W. H.; Le, K. P.; Grey, J.; Au, T. T.; Sail, M. J. *Science* **1997**, *276*, 1826.
(17) (a) Bekiari, V.; Lianos, P. *Langmuir* **1998**, *14*, 3459. (b) Bekiari, V.; Lianos, P. *Chem. Mater.* **1998**, *10*, 3777.

10.1021/cm035028z CCC: $27.50
Published on Web 03/19/2004

amine-functionalized cross-linked sol−gel derived hybrids involving essentially four alkoxysilane precursors, 3-isocyanatopropyltriethoxysilane (ICPTES), 3-glycidyloxypropyltriethoxysilane (GPTES), 3-glycidyloxypropyltrimethoxysilane (GPTMS), and 3-aminopropyltriethoxysilane (APTES). For instance, Green et al.[16] reported the synthesis of highly emissive phosphors synthesized from tetraalkoxysilane sol−gel precursors, such as tetramethoxysilane or APTES, and a variety of organic acids. These materials display a broad visible photoluminescence spectrum that appears white to the naked eye. In particular, it is worth mentioning that the APTES−formic acid hybrid, with an external photoluminescence (PL) quantum yield of 35 ± 1%,[16] is one of the most efficient phosphors known among those lacking activator metal ions. For APTES−acetic acid phosphors quantum yields of 21 and 12% were estimated for the two distinct emissions.[17]

Another family of amine-functionalized multiwavelength hybrid phosphors, extensively studied in the past few years, is obtained from urea [NHC(=O)NH] and urethane [NHC(=O)O] precursors. The basic structure of these xerogels, classed as di-ureasils and di-urethanesils, respectively, consists of a siliceous skeleton to which oligopolyether chains of different lengths are covalently grafted by means of urea[18−21,23,26−29] or urethane bridges.[30] The incorporation of lanthanide (e.g., europium) salts into the di-ureasil or di-urethanesil hybrid frameworks allows fine-tuning of the emission color across the CIE (Commission International de L'Eclairage) chromaticity diagram, by changing the amount of incorporated salt or the excitation wavelength.[29]

All these amide- or amine-functionalized sol−gel derived hybrids have been synthesized either by the conventional sol−gel method (e.g., in the presence of water and ethanol[18,20,23] and using inorganic acids, such as HCl, as the catalyst[19,21,22,24]) or by carboxylic acid solvolysis of alkoxides, in the absence of water and oxygen, using APTES or poly(oxypropylene) (POP) as precursors.[16,17,25−27] Compared to the hybrid materials obtained from the conventional sol−gel process, these hybrid materials derived from carboxylic acid solvolysis have the following advantages: (1) they are easily prepared; (2) they exhibit higher PL quantum yields;[16] and (3) the slow gelation process produces a compact and uniform gel without any entrapment of liquid favoring the performance of functional devices.[25]

The main goal of this paper is to demonstrate that solvolysis in the presence of carboxylic acids is a promising method to prepare optically functional poly(oxyethelene) (POE)-based di-ureasils and di-urethanesils with PL quantum yields substantially higher than those found in analogous hybrids obtained from conventional sol−gel process. The higher quantum yields of the hybrids prepared through carboxylic acid solvolysis, relative to those of di-ureasils and di-urethanesils synthesized via the conventional sol−gel technique, are discussed in terms of the hydrogen bonding established between adjacent urea or urethane cross-links. It should be stressed that although some work has recently been devoted to the study of di-ureasils carrying POP chains prepared by carboxylic acid solvolysis,[25−27] the structural similarity of these samples relative to those prepared by conventional sol−gel route and the determination of the PL quantum yields have not yet been reported. Furthermore, this paper reports for the first time the synthesis of di-urethanesils via carboxylic acid solvolysis, their structural characterization, and the determination of the PL quantum yields.

II. Experimental Section

Materials. The diamine α,ω-diaminepoly(oxyethylene-*co*-oxypropylene (commercially designated as Jeffamine ED-600, Fluka) with a molecular weight of about 600 g/mol−corresponding to approximately 8.5 (OCH_2CH_2) repeat units−was dried over molecular sieves (4 Å, 1.6 mm pellets, Aldrich) dried at 180 °C in vacuum for 2 h before use. Poly(ethylene glycol) (PEG-300, Aldrich), with a molecular weight of about 300 g/mol−corresponding to approximately 6 (OCH_2CH_2) units−was used as received. ICPTES (Fluka, 95%), acetic acid (AA, Aldrich, 99.7%), and valeric acid (VA, Aldrich, 99.0%) were used without further purification. Tetrahydrofuran (THF) and absolute ethanol (CH_3CH_2OH) were dried over molecular sieves at room temperature (RT).

Synthesis. The first stage of the synthesis of the di-ureasils (di-urethanesils) studied here involved the reaction in THF of the isocyanate group of the alkoxysilane precursor ICPTES with the terminal amine (hydroxyl) groups of the doubly functional diamine Jeffamine ED-600 (PEG(300)) to form a urea (urethane) cross-linked organic−inorganic hybrid precursor, so-called ureapropyltriethoxysilane (d-UPTES(600)) (urethanepropyltriethoxysilane (d-UtPTES(300))). In the second stage of the synthetic procedure, CH_3CH_2OH and AA/VA were added to d-UPTES(600) (d-UtPTES(300)) to yield the di-ureasils (di-urethanesils) (see Scheme 1). A typical synthetic procedure follows.

Step 1. Synthesis of the Di-ureasil (Di-urethanesil) Precursor d-UPTES(600) (d-UtPTES(300)). The procedure used was similar to that previously reported in the literature.[20,23,28,30] A volume of 2.38 mL (4.17 mmol) (2.00 mL (7.50 mmol)) of Jeffamine ED-600 (PEG-300) was dissolved in 10.0 mL of dried THF in a flask in a fume cupboard. A volume of 2.17 mL (8.34

(18) de Zea Bermudez, V.; Carlos, L. D.; Duarte, M. C.; Silva, M. M.; Silva, C. J. R.; Smith, M. J.; Assunção, M.; Alcácer, L. *J. Alloys Compd*. **1998**, *275*−*277*, 21.

(19) Ribeiro, S. J. L.; Dahmouche, K.; Ribeiro, C. A.; Santilli, C. V.; Pulcinelli, S. H. J. *J. Sol-Gel Sci. Technol.* **1998**, *13*, 427.

(20) (a) de Zea Bermudez, V.; Carlos, L. D.; Alcácer, L. *Chem. Mater.* **1999**, *11*, 569. (b) Carlos, L. D.; de Zea Bermudez V.; Sá Ferreira R. A.; Marques L.; Assunção M. *Chem. Mater.* **1999**, *11*, 581. (c) Sá Ferreira, R. A.; Carlos, L. D.; de Zea Bermudez V. *Thin Solid Films* **1999**, *343*, 470.

(21) (a) Bekiari, V.; Lianos, P.; Lavrencic-Stangar, U. L.; Orel, B.; Judenstein, P. *Chem. Mater.* **2000**, *12*, 3095. (b) Stathatos, E.; Lianos, P.; Lavrencic-Stangar, U.; Orel, B.; Judenstein, P. *Langmuir* **2000**, *16*, 8672.

(22) (a) Lin, J.; Baerner, K. *Mater. Lett.* **2000**, *46*, 86. (b) Han, Y.; Lin, J.; Zhang, H. *Mater. Lett.* **2002**, *54*, 389.

(23) Carlos, L. D.; Sá Ferreira R. A.; de Zea Bermudez V.; Ribeiro, S. I. L. *Adv. Funct. Mater.* **2001**, *11*, 111.

(24) Cordoncillo, E.; Guaita, F. J.; Escribano, P.; Philippe, C.; Viana, B.; Sanchez, C. *Opt. Mater.* **2001**, *18*, 309.

(25) Stathatos, E.; Lianos, P.; Lavrencic-Stangar, U.; Orel, B. *Adv. Mater.* **2002**, *14*, 354.

(26) Brankova, T.; Bekiari, V.; Lianos, P. *Chem. Mater.* **2003**, *15*, 1855.

(27) Stathatos, E.; Lianos, P.; Orel, B.; Vuk, A. S.; Jese, R. *Langmuir* **2003**, *19*, 7587.

(28) Carlos, L. D.; Sá Ferreira, R. A.; de Zea Bermudez, V. In *Handbook of Organic−Inorganic Hybrid Materials and Nanocomposites*; Nalwa, H. S., Ed.; American Scientific Publishers: Stevenson Ranch, CA, 2003; Vol. 1, Chapter 9, pp 353−380.

(29) (a) Carlos, L. D.; Sá Ferreira, R. A.; de Zea Bermudez, V.; Molina, C.; Bueno, L. A.; Ribeiro, S. J. L. *Phys. Rev. B* **1999**, *60*, 10042. (b) Carlos, L. D.; Messaddeq, Y.; Brito, H. F.; Sá Ferreira, R. A.; de Zea Bermudez, V.; Ribeiro, S. J. L. *Adv. Mater.* **2000**, *12*, 594, (c) Sá Ferreira, R. A.; Carlos, L. D.; Gonçalves, R. R.; Ribeiro, S. J. L.; de Zea Bermudez, V. *Chem. Mater.* **2001**, *13*, 2991.

(30) (a) Gonçalves, M. C.; de Zea Bermudez, V.; Ostrovskii, D.; Carlos, L. D. *Ionics* **2002**, *8*, 62. (b) de Zea Bermudez, V.; Ostrovskii, D.; Gonçalves, M. C.; Carlos, L. D.; Sá Ferreira, R. A.; Reis, L.; Jacobsson, P. *Chem. Phys. Phys. Chem.* **2004**, *6* (3), 638.

Scheme 1. Preparation of the Di-ureasils and Di-urethanesils through Carboxylic Acid Solvolysis

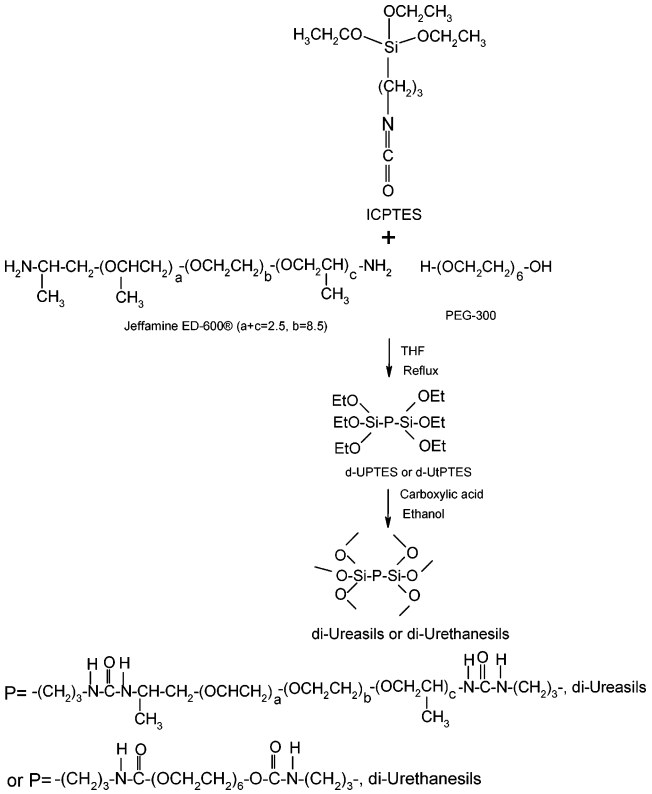

mmol) (3.90 mL (15.0 mmol)) of ICPTES was then added to this solution under stirring. The molar ratio of Jeffamine ED-600 (PEG(300)) to ICPTES was 1:2. The flask was sealed and the solution was stirred at RT (at about 350 K) in N_2 atmosphere for 24 h. The grafting process was infrared monitored through the observation of the progressive reduction and ultimate disappearance of the band located at 2274 cm^{-1}, attributed to the vibration of the $\equiv Si(CH_2)_3NCO$ group, and the growth of the band envelope characteristic of the urea (urethane) group (1800−1500 cm^{-1} interval).

Step 2. Synthesis of the Di-ureasils (Di-urethanesils). The mixture produced in the first step was heated in a water bath at about 45 °C under vacuum to allow the evaporation of THF. A transparent d-UPTES(600) (d-UtPTES(300)) oil was thus obtained. A volume of 1.95 mL (33.4 mmol) (3.50 mL (60.0 mmol)) of CH_3CH_2OH was then added to d-UPTES(600) (d-UtPTES(300)) (molar ratio ICPTES/CH_3CH_2OH = 1:4). The mixture was degassed and frozen at liquid nitrogen temperature (77 K) and submitted to three freeze−pump−thaw cycles to remove oxygen or any volatile impurities. A volume of 1.44 mL (25.0 mmol) (2.60 mL (45.0 mmol)) of AA or 2.75 mL (25.0 mmol) of VA (molar ratio of d-UPTES(600) (d-UtPTES(300))/carboxylic acid = 1:6) was then added in nitrogen atmosphere under stirring. The resulting mixture was stirred under the same conditions at ca. 40 °C for 3 (2) days. The sol formed was poured into a 70-mm-diameter Teflon mold covered with Parafilm with needle holes and dried at ambient conditions for several days until gelation occurred. We must stress that gelation did not occur if the samples were kept up in a nitrogen atmosphere for about 10 days. Di-ureasil and di-urethanesil xerogels were thus formed by exposure of the corresponding sols to ambient humidity. Lianos et al.[27] recently reported this evidence for the acetic acid solvolysis of analogous di-ureasils. The di-ureasil (di-urethanesil) produced was first dried at 50 °C to yield a transparent and colorless material, and then dried at 80 °C under vacuum to produce the final di-ureasil (di-urethanesil) hybrid, obtained as a transparent, fairly rigid, and elastomeric monolithic film, with a light yellow hue (almost colorless). This result is similar to that obtained by Bekiari et al., who noted that the gels prepared through the carboxylic acid solvolysis changed progressively from colorless to deep yellow-orange during the aging period.[17b] The di-ureasil derived from AA and VA solvolysis process were named d-U(600)-AA and d-U(600)-VA, respectively, whereas the di-ureasil obtained through the conventional sol−gel process was simply designated as d-U(600). Accordingly, the di-urethanesil prepared here and that synthesized through the conventional sol−gel method were named d-Ut(300)-AA and d-Ut(300), respectively.

Experimental Techniques. Mid-infrared spectra were recorded at RT using a MATTSON 7000 FTIR spectrometer. The spectra were collected over the range 4000−400 cm^{-1} by averaging 64 scans at a maximum resolution of 4 cm^{-1}. The compounds were finely ground (about 2 mg), mixed with approximately 175 mg of dried potassium bromide (Merck, spectroscopic grade) and pressed into pellets. Prior to recording the spectra the disks were stored in an oven under vacuum at 80 °C for several days in order to reduce the levels of byproduct, solvent, and adsorbed water. Consecutive spectra were recorded until reproducible results were obtained.

X-ray diffraction patterns were recorded using a Philips X'Pert MPD powder X-ray diffractometer system. The powders were exposed to the Cu Kα radiation (λ = 1.54 Å) at RT in a 2θ range (scattering angle) between 1 and 80°. The xerogel samples, analyzed as films, were not submitted to any thermal pretreatment.

^{29}Si magic-angle spinning (MAS) and ^{13}C cross-polarization (CP) MAS NMR spectra were recorded on a Bruker Avance 400 (9.4 T) spectrometer at 79.49 and 100.62 MHz, respectively. ^{29}Si MAS NMR spectra were recorded with 2-μs (equivalent to 30°) rf pulses, a recycle delay of 60 s, and a 5.0-kHz spinning rate. ^{13}C CP/MAS NMR spectra were recorded with 4-μs ^1H 90° pulses, 2-ms contact time, a recycle delay of 4 s, and a spinning rate of 8 kHz. Chemical shifts are quoted in ppm from TMS.

The emission (PL) and excitation (PLE) spectra were recorded on a modular double-grating excitation spectrofluorimeter with a TRIAX 320 emission monochromator (Fluorolog-3, Jobin Yvon-Spex) coupled to a R928 Hamamatsu photomultiplier. All the spectra, corrected for optics and detection spectral response, were measured in the front face acquisition mode at RT.

The absolute emission quantum yields (ϕ) were measured at RT using the technique for powdered samples described by Wrigthon et al.[31] and the following expression:

$$\phi = A/(R_S - R_H) \quad (1)$$

where A is the area under the di-ureasils or di-urethanesils emission spectra, and R_S and R_H are the diffuse reflectance (with respect to a fixed wavelength) of the hybrids and of the reflecting standard, respectively. Emission and diffuse reflectance spectra were corrected for the detector spectral response. As reflecting standard we used MgO, which has a reflectivity close to the unit (r = 91%). Powder size and packing fraction are crucial factors because R_S and R_H intensity depend on them. Thus, the diffuse reflectance was first measured at a wavelength not absorbed by the nanohybrids (720 nm). The di-ureasils and di-urethanesils were thoroughly ground until R_H totally overlapped with R_S, indicating a similar powder size and packing fraction. To prevent insufficient absorption of the exciting radiation, a powder layer around 3 mm was used and utmost care was taken to ensure that only the sample was illuminated, to diminish the quantity of light scattered by the front sample holder. Diffuse reflectance and emission spectra were recorded on a Jobin Yvon-Spex spectrometer (HR 460) coupled to a R928 Hamamatsu photomultiplier, using a perpendicular illumination of the sample. A Xe arc lamp (150 mW) coupled to a Jobin Yvon-Spex monochromator (TRIAX 180) was used as excitation source. All the spectra were

(31) Wrigton, M. S.; Ginley, D. L.; Morse, J. *Chem. Phys.* **1974**, *78*, 2229.

corrected for the response of the detector. The same experimental conditions, namely, position of the hybrids/standard holder, excitation and detection monochromator slits (0.3 and 0.1 mm, respectively) and optical alignment, were fixed. Several measurements were carried out for each sample, indicating reproducibility within 15%. However, the errors in the quantum yield values associated with this technique were estimated within 25%.[31]

The accuracy and reproducibility of our measurements were tested by measuring the ϕ value of sodium salicylate (Panreak, 99.5%), a commercial standard. Sodium salicylate presents a large broad band peaking around 425 nm, with a constant ϕ value (60%) for excitation wavelengths between 220 and 380 nm. These properties render sodium salicylate an adequate standard for ultraviolet absorbing samples, like in the di-ureasils and di-urethanesils. Five measurements were performed to determine the sodium salicylate quantum yield at 350 nm, using the described experimental setup. The values found are within the 65.9 ± 3.6% interval.

III. Results and Discussion

Mechanism of Carboxylic Acid Solvolysis. In the conventional sol−gel process, the hydrolysis process is initiated when alkoxides such as TEOS, d-UPTES(600), or d-UtPTES(300) react with water in the presence of an acidic or basic catalyst. As a result of this reaction, silicon hydroxyl groups, Si−OH, become attached to the precursor molecules. Two hydrolyzed molecules (or a nonreacted molecule and a hydrolyzed one) can link together through condensation of two Si−OH groups (or one Si−OH group and one Si−OR group, where R is an alkyl group) and release a small molecule, such as water (or alcohol). The larger silicon-containing molecules (i.e., the hybrid materials) are produced as the condensation reactions proceed through polymerization.[1,2] Alternatively, the silicon-based networks may be obtained through solvolysis of the precursors in the presence of ethanol and a carboxylic acid, such as acetic acid. At present, the mechanism of carboxylic acid solvolysis of the precursors in the presence of ethanol is not totally clear. The two-step reaction mechanism for this process, proposed by Pope and Mackenzie,[32] was recently confirmed by Lianos et al.[25] for the acetic acid solvolysis of POP(4000)/siloxane hybrids in the presence of ethanol using a temporal attenuated total reflection IR measurement technique. This mechanism has also been used to explain the experimental results when De Azevedo and Brondani focused on the development of polyaniline/silicate glass composites by means of formic acid (playing the role of both solvent and catalyst) through a sol−gel process.[33] In the first step, acetic acid attacks the alkoxy groups bonded to the silicon atom (C_2H_5OSi-), forming an ester ($CH_3COOSi-$). During the second step, this ester reacts with ethanol, producing ethyl acetate ($CH_3COOC_2H_5$) and Si−OH groups. Then condensation of two Si−OH groups, or one Si−OH group and one ethanol molecule, yields the Si−O−Si network. Very recent data from Lianos' work indicated that the pure acetic acid solvolysis of di-ureasil precursors is a very slow process, especially when the reaction is operated in a dry N_2 atmosphere.[27]

Powder X-ray Diffraction. The RT X-ray diffraction of di-ureasils d-U(600)-AA, d-U(600)-VA, d-U(600), and di-urethanesils d-Ut(300)-AA and d-Ut(300) are presented in Figure 1. The patterns of all the samples show a main peak centered at ca. 21.0−21.7° associated with ordering within the siloxane domains. The second-order of this peak appears as a broad weak hump around 39−44°. Accordingly, a structural unit distance of 4.2 ± 0.1 Å is obtained. In addition, a shoulder is clearly discerned between 12 and 14° in all the hybrids patterns. This feature, not reported before, is ascribed to other intra-siloxane domains in-plane ordering with a characteristic distance of ca. 7.0 ± 0.5 Å.

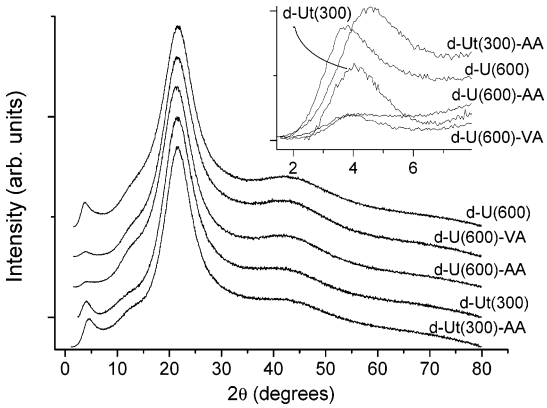

Figure 1. X-ray diffraction patterns of d-U(600), d-U(600)-AA, d-U(600)-VA, d-Ut(300), and d-Ut(300)-AA. The inset shows the X-ray diffractograms in the low 2θ region.

In an attempt to estimate the coherent length (L) over which the structural unit survives, the XRD patterns were fitted with pseudo-Voigt functions and the modified Scherrer equation

$$L = I\lambda/(A\cos\theta) \qquad (2)$$

where A, in radians, is the integrated area of the peaks and I is its intensity. Coherent lengths of 10 ± 2 and ca. 20−30 Å were obtained for the structural units distances of 4.2 and 7.0 Å, respectively. The former value is identical to that derived from small-angle X-ray scattering, for the dimension of the siliceous domains of analogous di-ureasils.[34]

The peak appearing at lower angles, ca. 3−4°, in the XRD patterns (inset of Figure 1) is due to interparticle scattering interference.[20b,34] From the peak maximum position (inset of Figure 1) we estimate an average interparticle distance of 24 ± 2 Å for d-U(600), and 23 ± 2 Å for d-U(600)-AA and d-U(600)-VA. The corresponding distances for d-Ut(300) and d-Ut(300)-AA are 20 ± 2 and 22 ± 2 Å, respectively. The similar values found for d-U(600)-AA and d-U(600)-VA indicate that these di-ureasils possess very similar nanostructures, despite the use of different carboxylic acids. XRD data point out strong structural similarity among the hybrids prepared by the two different methods. Indeed, the use of distinct carboxylic acids does not seem to induce significant differences in the hybrids' structures.

Fourier Transform Infrared Spectra (FT-IR). The FT-IR spectra of d-U(600)-AA, d-U(600)-VA, and d-Ut(300)-AA are shown in Figure 2A, whereas those

(32) Pope, E. J. A.; Mackenzie, J. D. *J. Non-Cryst. Solids* **1986**, *87*, 185.

(33) de Azevedo, W. M.; Brondani, D. J. *J. Non-Cryst. Solids* **2001**, *296*, 224.

(34) (a) Dahmouche, K.; Santilli, C. V.; Pulcinelli, S. H.; Craievich, A. F. *J. Phys. Chem. B* **1999**, *103*, 4937. (b) Dahmouche, K.; Carlos, L. D.; De Zea Bermudez, V.; Sá Ferreira, R. A.; Santilli, C. V.; Craievich, A. F. *J. Mater. Chem.* **2001**, *11*, 3249.

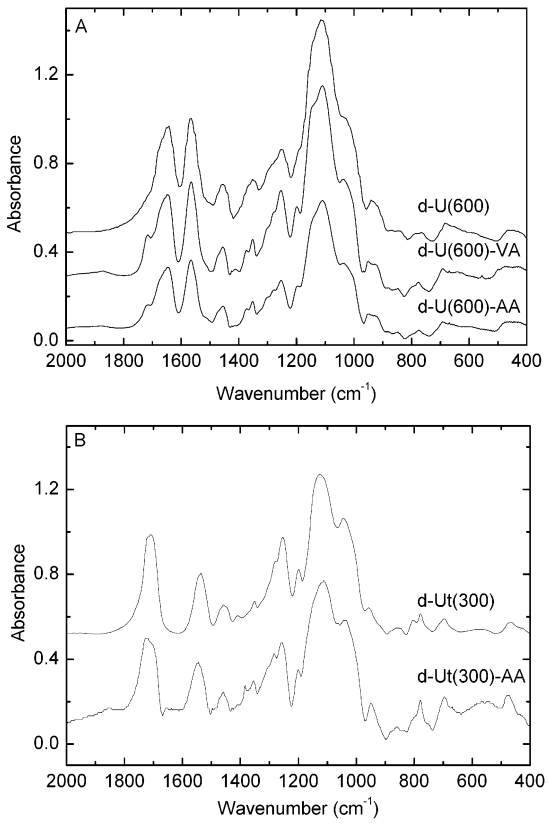

Figure 2. FT-IR spectra (2000−400 cm^{-1} range) of (A) d-U(600), d-U(600)-AA, d-U(600)-VA; and (B) d-Ut(300) and d-Ut(300)-AA.

of d-Ut(300)-AA and d-Ut(300) are represented in Figure 2B. The frequency, intensity, and attributions of the bands are given in Tables 1 and 2.

d-U(600)-AA and d-U(600)-VA Di-ureasils. The FT-IR spectra of d-U(600)-AA and d-U(600)-VA obtained from the solvolysis method are essentially the same as that of the di-ureasil d-U(600) derived from the conventional sol−gel process (Figure 2A, Table 1).[20a] It is of interest to note that the bands at 1324 cm^{-1} in the spectrum of d-U(600)-AA and at 1323 cm^{-1} in that of d-U(600)-VA are characteristic of the amorphous state.[20a] The shoulders at 922 and 924 cm^{-1} in the spectra of for d-U(600)-AA and d-U(600)-VA, respectively, provide additional evidence that in the solvolysis-derived di-ureasils the POE chains attain complete disorder. These results are consistent with the results reported previously for d-U(600).[20a]

Important differences between the di-ureasils synthesized through the conventional and nonconventional methods are observed in the region of the urea groups vibrations, the so-called "amide I" (1800−1600 cm^{-1}) and "amide II" regions (1600−1500 cm^{-1}). The "amide I" mode is a highly complex vibration involving the contribution of the C═O stretching, the CN stretching, and the C−C−N deformation.[35] To study in detail the "amide I" band of the di-ureasils, spectral deconvolution was carried out in the 1760−1610 cm^{-1} range using the Origin package and Gaussian band shapes (Table 3). Three components were isolated for the "amide I" envelope of d-U(600)-AA and d-U(600)-VA, at 1719, 1668, and 1640 cm^{-1}, and at 1717, 1669, and 1640 cm^{-1}, respectively. The components at ca. 1720 and 1670 cm^{-1} are due to the vibration of urea-polyether hydrogen-bonded structures, whereas the component at about

(35) Skrovanek, D. J.; Howe, S. E.; Painter, P. C.; Coleman, M. M. *Macromolecules* **1985**, *18*, 1676. (b) Coleman, M. M.; Lee, K. H.; Skrovanek, D. J.; Painter, P. C. *Macromolecules* **1986**, *19*, 2149.

Table 1. FT-IR Spectra of d-U(600), d-U(600)-AA, and d-U(600)-VA[a]

d-U(600) (ref 20a)	d-(600)-AA	d-(600)-VA	attributions (ref 20a)
3351 m	3349 m	3344 m	ν NH hydrogen-bonded
3116 w	3111 w	3115 w	
2965 sh	2965 sh	2967 sh	ν_a CH_3
2931 s	2931 s	2932 s	ν_a CH_2
2873 s	2873 s	2876 s	ν_s CH_2
2748 sh	2747 sh	2747 sh	combination vibration
1715 sh	1718 sh	1716 m	"amide I"
1671 sh	1673 sh	1671 sh	
1642 s	1646 s	1646 s	
1565 s	1566 s	1565 s	"amide II"
1476 sh	1472 sh	1471 sh	CH_2 scissoring and CH_3 deformation
1455 m	1456 m	1456 m	
1373 m	1373 m	1373 m	CH_2 wagging
1351 m	1353 m	1353 m	
1322 w	1324 w	1323 w	liquid state
1301 m	1301 sh	1301 sh	
1276 m	1276 m	1278 m	"amide III"
1253 m	1253 m	1254 m	CH_2 twisting
1193 m	1194 m	1198 m	
1151 sh	1143 sh	1145 sh	ν CO + rCH_2
1110 vs	1110 S	1109 S	ν CO
1037 m	1037 m	1037 m	ν CO, ν CC, rCH_2
950 w	949 w	949 w	ν CC, rCH_2
921 sh	922 sh	924 sh	liquid state
879 vw	882 vw	882 vw	ν CO, rCH_2
850 m	849 w	848 w	
790 vw	790 sh	790 sh	
775 vw	775 vw	776 vw	"amide VI"
692 vw	691 vw	691 vw	"amide V"
669 vwb	669 vw	669 vw	
472 vwb	468 vwb		COC + CCO bending

[a] Frequencies in cm^{-1}; vs, very strong; m, medium; w, weak; vw, very weak; sh, shoulder; b, broad.

Table 2. FT-IR Spectra of d-Ut(300) and d-Ut(300)-AA[a]

d-Ut(300)	d-Ut(300)-AA	attributions
3507 sh	3505 sh	
	3370 m	adsorbed water
3337 m		
2937 s	2932 s	ν_a CH_2
2880 s	2879 s	ν_s CH_2
		combination vibrations
1719 sh	1722 s	"amide I"
1709 s	1710 s	
		adsorbed water
1536 m	1545 m	"amide II"
1457 m	1459 m	CH_2 scissoring and CH_3 deformation
1351 w	1354 w	CH_2 wagging
		liquid state
1280 sh	1284 sh	"amide III"
1253 m	1257 m	CH_2 twisting
1200 w	1200 w	
1123 vs	1120 vs	νCO
1042 s	1038 s	νCO + rCH_2
954 w	949 w	νCC, rCH_2
856 w	860 w	νCO, rCH_2
806 w	804 w	liquid state
778 w	779 w	
696 w	696 w	
	564	
468 w	475 w	

[a] Frequencies in cm^{-1}; vs, very strong; m, medium; w, weak; vw, very weak; sh, shoulder; b, broad.

Table 3. Curve-Fitting Results of "Amide I" Region in the FT-IR Spectra for d-U(600)-AA, d-U(600)-VA, d-U(600), d-Ut(300)-AA, and d-Ut(300)

di-ureasils and di-urethanesils	frequency (cm^{-1})/area (%)			
d-U(600)-AA		1719/(17)	1668/(57)	1640/(26)
d-U(600)-VA		1717/(24)	1669/(54)	1640/(22)
d-U(600)		1720/(8)	1671/(54)	1639/(38)
d-Ut(300)-AA	1756/(17)	1723/(64)	1694/(19)	
d-Ut(300)	1735/(41)	1723/(22)	1699/(37)	

1640 cm^{-1} results from the formation of strong self-associated hydrogen-bonded urea−urea associations.[20a,36] The absence of an individual band at 1750 cm^{-1} in the spectra of d-U(600)-AA or d-U(600)-VA indicates that neither C═O nor N−H groups are left free in the hybrid materials, in agreement with the situation reported for d-U(600).[20a,36] The presence of larger quantities of urea−urea associations in d-U(600) than in d-U(600)-AA or d-U(600)-VA will be connected in the PL Section with the increase of the PL quantum yields of the latter two hybrids relative to the former one.

The temperature dependence of the di-ureasils' FT-IR spectra in the high-frequency region and in the "amide I" region was also investigated (not shown). The broad band observed at ca. 3500 cm^{-1} is assigned to molecular water absorbed on the surface of the materials, although the contribution of the vibration associated with silanol groups cannot be excluded. Absorbed water is known to give a characteristic peak at about 1650 cm^{-1}. As expected, the intensity of the bands at 3500 and 1650 cm^{-1} decrease gradually with the increase of temperature. The former feature almost disappeared after a certain heating time, indicating that all the water absorbed in the materials had been successfully removed. In parallel, the intensity of the band at about 1656 cm^{-1} decreased significantly. These changes were accompanied by the decrease of the intensity of the 1720 cm^{-1} peak and the increase of the intensity of the 1670 and 1640 cm^{-1} bands, proof that the withdrawal of water through heating led to the formation of a larger number of strong hydrogen-bonded associations.

The "amide II" mode is a mixed contribution of the N−H in-plane bending, C−N stretching, and C−C stretching vibrations.[35] This band appears at 1566 and 1565 cm^{-1} in the spectra of d-U(600)-AA and d-U(600)-VA, respectively, the exact position found in the case of d-U(600) (Figure 2A, Table 1).

d-Ut(300)-AA Di-urethanesil. Figure 2B shows that the FT-IR spectrum of d-Ut(300)-AA derived from solvolysis closely resembles that of the d-Ut(300) hybrid prepared through the conventional sol−gel process (Table 2). Deconvolution of the "amide I" band of d-Ut-(300)-AA (Table 3) yields three distinct components centered at 1756, 1722, and 1694 cm^{-1}, almost exactly where the d-Ut(300) (Table 2) bands are found. The band at 1755 cm^{-1} is due to the free carbonyl moieties of the urethane cross-links with no hydrogen bonding interactions, whereas the band at 1721 cm^{-1} is ascribed to the vibration of hydrogen-bonded urethane−polyether associations.[30] The band at 1693 cm^{-1} is assigned to a self-associated hydrogen-bonded urethane−urethane structure.[30] As demonstrated in Table 3, there is a larger quantity of self-associated urethane−urethane associations in d-Ut(300) than in d-Ut(300)-AA. This will be related in the PL Section to the increase of the quantum yield of Ut(300)-AA relative to that of d-Ut-(300).

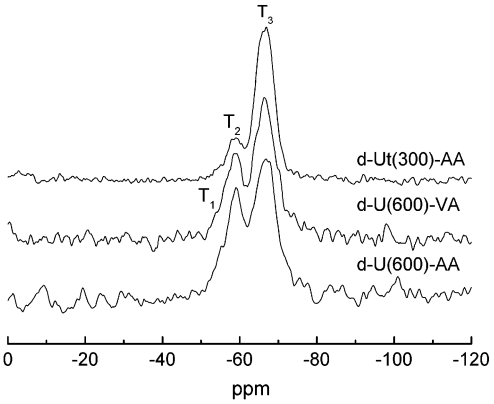

Figure 3. ^{29}Si MAS NMR spectra of d-U(600)-AA, d-U(600)-VA, and d-Ut(300)-AA.

^{29}Si MAS NMR. The ^{29}Si MAS NMR spectra of d-U(600)-AA, d-U(600)-VA, and d-Ut(300)-AA exhibit broad signals characteristic of T_1, T_2, and T_3 units (Figure 3). These sites are labeled using the conventional T_n notation, where n (n = 1, 2, 3) is the number of Si-bridging oxygen atoms. The T_2 and T_3 environments (at −59 and −67 ppm, respectively) are clearly dominant, showing the presence of two main types of local structures: $(SiO)_2Si(CH_2)_3OH$ and $(SiO)_3Si(CH_2)_3$. The shoulder displayed by some of the hybrids at ca. −50 ppm is ascribed to T_1 sites.

The peak positions for d-U(600)-AA, d-U(600)-VA, and d-Ut(300)-AA and their relative population of the various silicon sites quantitatively estimated after deconvolution are presented in Table 4. The corresponding values already reported for d-U(600) and d-Ut(300)[37] are also listed for comparison. The degree of condensation, c (Table 4), was calculated using the expression

$$c = \frac{1}{3}(\%T_1 + 2\%T_2 + 3\%T_3) \qquad (3)$$

The values obtained, about 83% for d-U(600)-AA, 86% for d-U(600)-VA, and 93% for d-Ut(300)-AA, are similar to those reported for the corresponding hybrids prepared by the conventional sol−gel process,[37] and highlight the structural similarity of these materials.

^{13}C CP MAS NMR. The ^{13}C MAS NMR spectra of d-U(600)-AA, d-U(600)-VA and d-U(600) are shown in Figure 4A. The assignments of the resonances are given in Table 5. It is useful to examine some features of the ^{13}C MAS NMR spectra reported in the literature for analogous materials. While studying polysiloxane-immobilized amine ligand systems El Nahhal et al. reported that the spectra of APTES exhibited three signals at about 11.2, 24.8, and 43.6 ppm due to the methylene carbons and two signals at 58.1 and 17.6 ppm associated with the ethoxy carbons.[38] Davis et al. detected signals at about 11, 25, 45, 52, 73, and 75 ppm for the six

(36) de Zea Bermudez, V.; Sá Ferreira, R. A.; Carlos, L. D.; Molina, C.; Dahmouche, K.; Ribeiro, S. J. L. *J. Phys. Chem. B* **2001**, *105*, 3378.

(37) Carlos, L. D.; Sá Ferreira, R. A.; Orion, I.; de Zea Bermudez, V.; Rocha, J. *J. Lumin.* **2000**, *87*−*89*, 702.

(38) El Nahhal, I. E.; Chehimi, M. M.; Cordier, C.; Dodin, G. *J. Non-Cryst. Solids* **2000**, *275*, 142.

Table 4. ^{29}Si MAS NMR Spectra Chemical Shifts (ppm), Population of the Different T_n Species (%), and Degree of Condensation, *c*, of the Di-Ureasils or Di-Urethanesils Synthesized through Carboxylic Acid Solvolysis[a]

	T_1 R′Si(OSi)(OR)$_2$ (%)	T_2 R′Si(OSi)$_2$(OR) (%)	T_3 R′Si(OSi)$_3$ (%)	*c* (%)	ref
d-U(600)		−59.5 (13)	−67.4 (87)	96	37
d-U(600)-AA	−55.5 (11)	−58.9 (28)	−66.9 (61)	83	
d-U(600)-VA	−55.5 (11)	−58.9 (19)	−66.5 (70)	86	
d-Ut(300)	−49.2 (2)	−58.2 (41)	−66.6 (57)	85	37
d-Ut(300)-AA	−54.1 (2)	−58.5 (16)	−66.3 (82)	93	

[a] R denotes hydrogen or ethyl groups and R′ denotes the ureapropyl or urethanepropyl chains.

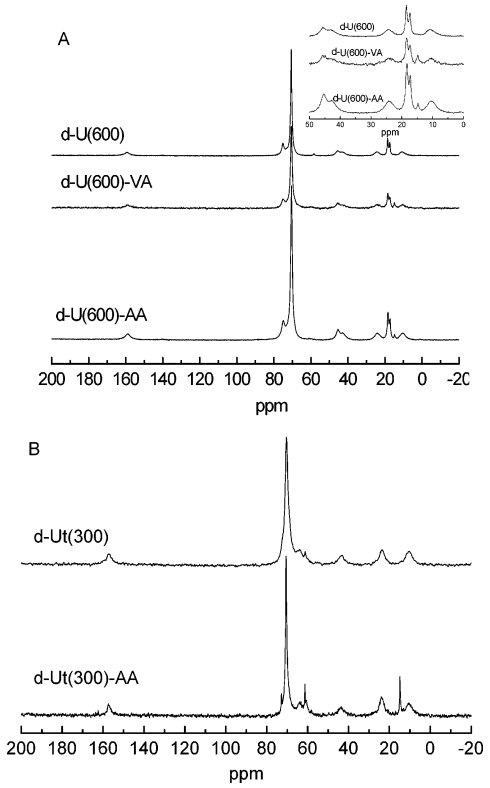

Figure 4. ^{13}C CP/MAS NMR spectra of (A) d-U(600), d-U(600)-AA, d-U(600)-VA; and (B) d-Ut(300) and d-Ut(300)-AA.

carbons of the GPTMS precursor of epoxy/silica hybrids.[39] Ribot et al. attributed a peak at 71 ppm to PEG (−OCH_2CH_2−), the signal at 175 ppm to the carboxylate moiety, and the peaks between 10 and 30 ppm to carbon atoms belonging to butyl groups.[40] The sol−gel derived hybrid materials synthesized by Franville et al. displayed the characteristic $(CH_2)_3$ resonances at 43, 23, and 11 ppm, and the C═O amide functions at 164 ppm.[41] Chang et al. assigned the peaks around 41, 22, and 15 ppm to −NCH_2−, −CH_2−, and −CH_2Si− groups, respectively.[42] Finally, Lindner et al. attributed the signals at 68 and 58 ppm to −CH_2O− and CH_3O− groups, respectively.[43]

On the basis of the assignments proposed by the authors mentioned above, the strongest peak at ca. 70.5 ppm in the ^{13}C MAS NMR spectra of the di-ureasils d-U(600)-AA, d-U(600)-VA, and d-U(600) (Figure 4A) is attributed to −(OCH_2CH_2)− groups of the polymer chains, whereas the shoulders at about 75 ppm are very likely given by −OCH groups (Table 5). The peaks at ca. 45 (with a shoulder at about 43 ppm), 24, and 10.5 ppm are characteristic of the $(CH_2)_3$ aliphatic chains (Table 5). The low field peak at approximately 159 ppm is associated with the urea C═O groups. The signal at 17.4 ppm is assigned to different −CH_3 groups of the polymer chains. The faint resonances at 58.2 and 17.4 ppm and at 58.0 and 18.3 ppm in the spectra of d-U(600) and d-U(600)-AA, respectively, (Table 5) are characteristic of carbons ethoxy groups. This suggests that most ethoxy groups are hydrolyzed into Si−OH moieties, which condense, yielding d-U(600)-AA and d-U(600)-VA.

Although the di-urethanesils d-Ut(300)-AA and d-Ut(300) exhibit fewer peaks in the ^{13}C MAS NMR spectra than the di-ureasils, the spectra are globally very similar (Figure 4B, Table 5). This confirms that the structures of d-Ut(300)-AA and d-Ut(300) are very similar.

Photoluminescence Spectra. Figure 5 shows the PL spectra of the di-ureasils d-U(600)-AA and d-U(600)-VA and the di-urethanesil d-Ut(300)-AA recorded at three selected excitation wavelengths. The spectra of the hybrids synthesized by the conventional sol−gel method, d-U(600) and d-Ut(300), are not shown, because they resemble those presented in Figure 5. For all hybrids, the emission spectra display a large broad band between 350 and 680 nm. The emission peak position strongly depends on the excitation wavelength, with a red-shift of the PL spectra being observed as the excitation wavelength increases from 350 to 420 nm.

As already reported, the large broad band results from the convolution of two emission components, in the blue and in the purple-blue spectral regions, peaking around 2.5−2.6 eV and 2.7−3.1 eV, respectively.[20b,23,28] The emission peak position of the former band is independent of the excitation wavelength, in contrast with the energy of the purple-blue band. The energy red-shift of the emission with the increasing of the excitation wavelength is described by: (i) a linear regime, characterized by a slope of ca. 0.5 between the emission peak position and the excitation energy, and (ii) a saturation regime, in which the emission peak position is independent of the excitation wavelength.[20c,28]

The nature of these two distinct emissions was investigated in detail by carefully considering the structure and PL properties of the hybrids and respective precursors, namely, diamines, PEG, d-UPTES(600), and d-UtPTES(300).[23,28] The blue and the purple-blue bands are ascribed to radiative electron−hole recombinations mediated by a mechanism typical of donor−acceptor pairs, occurring in the NH groups of the urea and urethane linkages and in the siliceous nanodomains, respectively. As far as the physical mechanism

(39) Davis, S. R.; Brough, A. R.; Atkinson, A. *J. Non-Cryst. Solids* **2003**, *315*, 197.
(40) Ribot, F.; Lafuma, A.; Eychenne-Baron, C.; Sanchez, C. *Adv. Mater.* **2002**, *14*, 1496.
(41) Franville, A. C.; Mahiou, R.; Zambon, D.; Cousseins, J. C. *Solid State Sci.* **2001**, *3*, 211.
(42) Chang, T. C.; Wang, G. P.; Tsai, H. C.; Hong, Y. S.; Chiu, Y. S. *Polym. Degrad. Stab.* **2001**, *74*, 229.
(43) Lindner, E.; Jäger, A.; Wegner, P.; Mayer, H. A.; Benez, A.; Adam, D.; Plies, E. *J. Non-Cryst. Solids* **1999**, *255*, 208.

Table 5. ^{13}C MAS NMR Chemical Shifts (ppm) and Their Assignments for d-U(600)-AA, d-U(600)-VA, d-U(600), d-Ut(300)-AA, and d-Ut(300)

d-U(600)	d-U(600)-AA	d-U(600)-VA	d-Ut(300)	d-Ut(300)-AA	assignments
159.3 w	158.8 w	158.9 w	157.1 w	157.4 w	−N(CO)N−
75.1 m	74.9 m	75.0 m			−OCH
70.6 vs	70.5 vs	70.6 vs	70.2 vs	70.5 vs	$-(OCH_2CH_2)-$
			63.7 w	63.9 w	
58.2 w	58.0 vw		61.1 w	61.3 w	$-CH_2-$ in $(CH_3CH_2O)_3Si-$
45.5 m	45.3 m	45.5 m	43.0 w	43.6 w	$-NCH_2-$ in $-N(CH_2)_3Si-$
43.0 sh	42.8 sh	42.5 sh			
24.3 m	24.2 m	23.9 m	23.5 m	23.9 m	$-CH_2-$ in $-N(CH_2)_3Si-$
18.5 s	18.4 s	18.4 s			$-CH_3-$ in $-(OCH_2CH(CH_3)-$
17.4 sh	17.3 sh	17.4 sh			$-CH_3-$ in $(CH_3CH_2O)_3Si-$
	14.8 w	14.8 w			
10.8 m	10.4 m	10.4 m	10.4 m	10.5 m	$-CH_2Si-$ in $-N(CH_2)_3Si-$

vs, very strong; s, strong; m, medium; w, weak; vw, very weak; sh, shoulder.

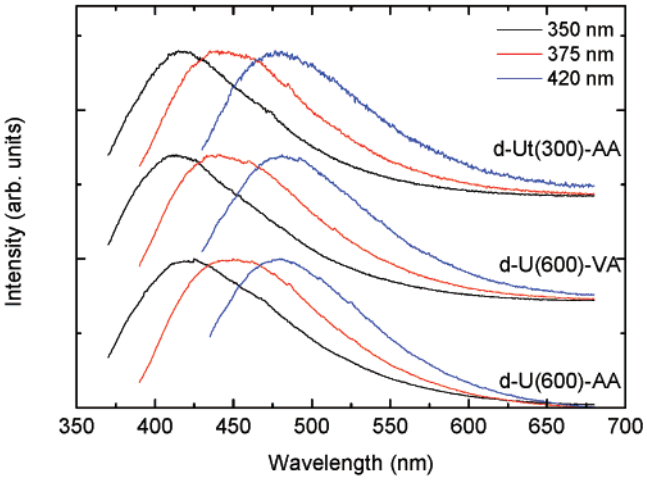

Figure 5. PL spectra of d-U(600)-AA, d-U(600)-VA, and d-Ut(300)-AA recorded at different excitation wavelengths.

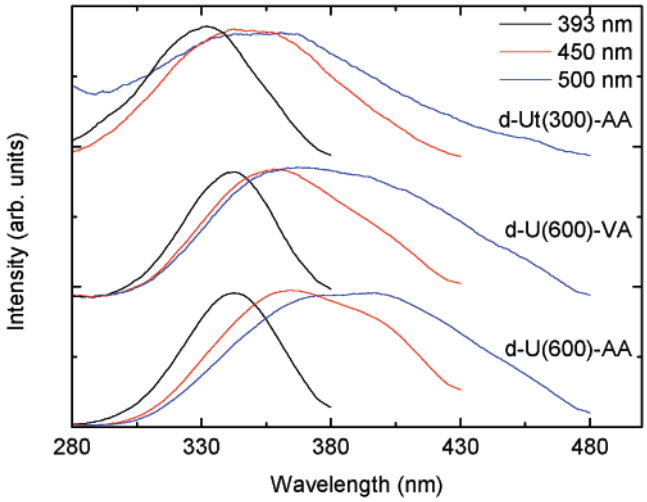

Figure 6. PLE spectra of d-U(600)-AA, d-U(600)-VA, and d-Ut(300)-AA monitored at different emission wavelengths.

behind the NH-related emission is concerned, we have recently proposed the photoinduced proton transfer between defects, such as NH_2^+ and N^- for the di-ureasils and the di-urethanesils.[28] The strong dependence of the purple-blue emission energy on the excitation wavelength has been already discussed.[28] This PL property is characteristic of all the materials (diamines, non-hydrolyzed precursors, di-ureasils, and di-urethanesils) under analysis, providing strong evidence of disordered-related processes generally associated with transitions between localized states in noncrystalline structures (e.g., porous silicon,[44] hydrogenated amorphous Si,[45] and As_2Se_3 glasses[46]). An identical dependence was also reported for a non-hydrolyzed di-ureasil precursor[21a] and for APTES-based hybrids with carboxylic acids.[17] The physical origin of such behavior is not entirely clarified, but it has been suggested that it may arise from radiative electron−hole recombination involving localized states within the conduction and valence bands.[23,28]

The PLE spectra were monitored along the hybrids' emission band, as shown in Figure 6 for d-U(600)-AA and d-U(600)-VA hybrids. The spectra consist of a strong broad band between 290 and 480 nm and no significant differences are observed in the PLE features of the two di-ureasils (paralleling the emission spectra conclusions). As the monitoring wavelength increases from 393 to 500 nm, the PLE spectra peak position shifts to the red and its full-width-at-half-maximum (fwhm) increases from 0.38 to 0.74 eV. The increased fwhm suggests the presence of more than one component, which is also indicated by the structured profile of the PLE spectra, for detection wavelengths higher than 393 nm. The presence of more than one component is obvious from the PLE spectra of d-U(600).[28] For the shorter monitoring wavelength (393 nm) the spectrum displays a broad band for which a peak position occurs around 359 nm (3.45 eV). When the detection wavelength is increased, the fwhm increases and another component clearly appears at low energy, centered at ca. 410 nm (3.02 eV).[28] The relative intensity of this band (but not the energy) increases with increasing monitoring wavelength. In contrast, the peak position of the more intense band shifts to the red as the detection varies from 393 to 550 nm. The presence of more than one component has been observed previously in the low-temperature (14 K) PLE spectra of the conventional di-ureasils[20b] and in the PLE spectra of two series' of Eu^{3+}-based di-ureasils.[29a] The lower and higher energetic bands were assigned to the preferential excitation of the blue (NH groups) and purple-blue (siliceous domains) emission bands, respectively.[23,28] Comparing the PLE features of the di-ureasils prepared through

(44) Sinha, S.; Banerjee, S.; Arora, B. M. *Phys. Rev. B* **1994**, *49*, 5706.
(45) Shah, J.; Pinczuk, A.; Alexander, F. B. *Solid State Commun.* **1982**, *42*, 717.
(46) Shah, J.; Bridenbaugh, P. M. *Solid State Commun.* **1980**, *34*, 101.

carboxylic acid solvolysis and by the conventional sol−gel process, the main difference is observed in the relative intensity of the bands. Whereas the component associated with the preferential excitation of the NH groups is more intense than that corresponding to the excitation of the siliceous domains in the former hybrids, the opposite is observed in the conventional di-ureasils. This indicates that the solvolysis process favors the NH-related emission.

The PLE spectra of d-Ut(300)-AA (Figure 6) show a large broad band in the same spectral region observed for the di-ureasils. The changes in the spectra observed with increasing monitoring wavelength are essentially the same as those described in the previous paragraphs for the di-ureasils prepared through carboxylic acid solvolysis. Moreover, such PLE properties, in particular the higher relative intensity of the NH-related component, are also observed in the d-Ut(300) hybrid prepared through solvolysis, in opposition to what has been observed with the di-ureasils. In the di-urethanesils family the luminescent properties do not depend on the synthesis procedure.

The smaller contribution of the NH groups to the PL features of the conventional d-U(600) relative to the d-Ut(300) and d-Ut(300)-AA may be induced by the stronger hydrogen bonds established between adjacent urea groups that do not occur in the urethane linkages, as pointed out by the above FTIR results. The number of hydrogen donor sites present in the urethane and urea groups is not the same: the urethane linkage contains just one NH group, whereas the urea moiety is composed of two NH groups. Thus, although the C═O moiety of a urethane group may form a single hydrogen bond with the NH moiety of another urethane group, urea groups of neighbor molecules may be linked by means of planar bifurcated hydrogen bonds.[47] As a consequence, the hydrogen bonding geometry of the urethane and urea groups may be significantly different. This results, for instance, in the tighter packing of adjacent chains observed in bis-urea compounds with respect to the bis-urethane analogues.[47a] The presence of stronger hydrogen bonds contributes to localizing the proton rendering difficult the induced transfer of hydrogen atoms between NH groups, and, consequently, the NH-related emission will be less intense in the d-U(600) sample.

Focusing now the discussion on the di-ureasils prepared through carboxylic acid solvolysis, the FTIR results suggest a decrease in the hydrogen interactions between urea linkages, which may account for the relative improvement of the luminescence properties associated with the NH groups. Hence, we conclude that the solvolysis process disfavors the formation of such type of strong interactions between urea groups although, at present, we cannot offer a good explanation for this. We should point out that the di-ureasil prepared with valeric acid has a lower number of urea groups involved in the hydrogen bonds (Table 3).

Emission Quantum Yields. Whereas the photoluminescent features of the di-ureasils and di-urethanesils prepared by the conventional sol−gel process and by carboxylic acid solvolysis are similar, an increase in the absolute emission quantum yield may be expected, following the previous discussion on the increase in the NH related emission, promoted by the solvolysis process. Indeed, Brankova et al. suggested this increase for related di-ureasils carrying POP chains.[26] To verify and quantify this point, the emission quantum yields of d-U(600), d-U(600)-AA, d-U(600)-VA, d-Ut(300), and d-Ut(300)-AA were measured for the excitation wavelength corresponding to the peak intensity maximum in the respective PLE spectrum. Table 6 lists the calculated ϕ values. Within experimental error, the measured quantum yields of the d-U(600) and d-Ut(300) hybrids are the same as those previously reported.[24] The ϕ values determined for the hybrids prepared through carboxylic acid solvolysis are always higher than those measured for the di-ureasils and di-urethanesils synthesized via the conventional sol−gel technique. Increases in ϕ between 27 and 33% and 35% were observed for the di-ureasils and di-urethanesils, respectively. Among the di-ureasils prepared through carboxylic acid solvolysis, there was a small increase (8%) in the quantum yield of the sample prepared with valeric acid. Although this increase is within the experimental error, it supports the importance, for improving luminescence properties, of reducing the strong hydrogen bonds between urea groups, as d-U(600)-VA displays a smaller number of NH groups involved in such type of cross-links.

Table 6. RT Absolute Emission Quantum Yields (%) for the Di-ureasils and Di-urethanesils Prepared by the Conventional Sol−Gel Process and by Carboxylic Acid Solvolysis[a]

d-U(600) (375 nm)	d-U(600)-AA (375 nm)	d-U(600)-VA (375 nm)	d-Ut(300) (400 nm)	d-Ut(300)-AA (400 nm)
6.6	9.6	10.4	12.0	19.7

[a] Numbers in parentheses indicate the excitation wavelength used.

IV. Conclusions

Di-ureasils d-U(600)-AA and d-U(600)-VA, and di-urethanesil d-Ut(300), were prepared through acetic acid and valeric acid solvolysis, and their structures and optical features were compared with those of similar hybrid materials prepared through the conventional sol−gel process. XRD, FT-IR, and ^{29}Si and ^{13}C MAS/NMR point out that the nanohybrids synthesized through solvolysis are structurally similar to the materials prepared via the conventional sol−gel route. The d-U(600)-AA, d-U(600)-VA, and d-Ut(300)-AA organic/inorganic hybrids are efficient RT white-light emitters, presenting an emission large broad band in the blue/purple−blue spectral region, similar to that previously reported for the d-U(600) and d-Ut(300) hybrids. Relative to these latter materials, the PL quantum yields of the hybrids prepared through carboxylic acid solvolysis increase around 30−35%. This effect was attributed to the presence of a lower proportion of self-associated hydrogen-bonded urea−urea and urethane−urethane associations in the hybrids prepared through carboxylic acid solvolysis, which contributes to delocalizing the proton and renders easy the induced transfer of hydro-

(47) (a) Born, L.; Hespe, H. *Colloid Polym. Sci.* **1985**, *263*, 335. (b) Chang, Y.-L.; West, M.-A.; Fowler, F. W.; Lauher, J. W. *J. Am. Chem. Soc.* **1993**, *115*, 5991. (c) De Loos, M.; van Esch, J.; Stokroos, I.; Kellogg, R. M.; Feringa, B. L. *J. Am. Chem. Soc.* **1997**, *119*, 12675. (d) van Esch, J.; Kellogg, R. M.; Feringa, B. L. *Tetrahedron Lett.* **1997**, *38*, 281.

gen atoms between adjacent NH groups, favoring, thus, the NH-related emission. Therefore, the present work supports that the carboxylic acid solvolysis synthesis process is a promising non-hydrolytic route for developing functional luminescent hybrids with potential applications in photonic and integrated optics. Furthermore, the optical functionality (in particular the external quantum yields) is determined by the extent and magnitude of the supramolecular interactions resulting from the self-assembly of urea or urethane groups via hydrogen bonding.

Acknowledgment. This work was supported by FEDER and Fundação para a Ciência e Tecnologia (FCT), POCTI/CTM/33653/00 and POCTI/CTM/46780/02. L.F. and N.J.O.S. thank FCT for postdoctoral (SFRH/BPD/5657/2001) and PhD grants (SFRH/BD/10383/2002), respectively. We acknowledge I. S. Gonçalves and J. A. Fernandes from the Chemistry Department of University of Aveiro for their help in the carboxylic acid solvolysis synthesis.

CM035028Z